

Accepted Manuscript

Hydroxy-substituted *trans*-cinnamoyl derivatives as multifunctional tools in the context of Alzheimer's disease

Angela De Simone, Manuela Bartolini, Andrea Baschieri, Kim Y.P. Apperley, Huan Huan Chen, Melissa Guardigni, Serena Montanari, Tereza Kobrlova, Ondrej Soukup, Luca Valgimigli, Vincenza Andrisano, Jeffrey W. Keillor, Manuela Basso, Andrea Milelli



PII: S0223-5234(17)30580-9

DOI: [10.1016/j.ejmech.2017.07.058](https://doi.org/10.1016/j.ejmech.2017.07.058)

Reference: EJMECH 9621

To appear in: *European Journal of Medicinal Chemistry*

Received Date: 15 March 2017

Revised Date: 29 May 2017

Accepted Date: 24 July 2017

Please cite this article as: A. De Simone, M. Bartolini, A. Baschieri, K.Y.P. Apperley, H.H. Chen, M. Guardigni, S. Montanari, T. Kobrlova, O. Soukup, L. Valgimigli, V. Andrisano, J.W. Keillor, M. Basso, A. Milelli, Hydroxy-substituted *trans*-cinnamoyl derivatives as multifunctional tools in the context of Alzheimer's disease, *European Journal of Medicinal Chemistry* (2017), doi: 10.1016/j.ejmech.2017.07.058.

This is a PDF file of an unedited manuscript that has been accepted for publication. As a service to our customers we are providing this early version of the manuscript. The manuscript will undergo copyediting, typesetting, and review of the resulting proof before it is published in its final form. Please note that during the production process errors may be discovered which could affect the content, and all legal disclaimers that apply to the journal pertain.

Hydroxy-substituted *Trans*-cinnamoyl Derivatives as Multifunctional Tools in the Context of Alzheimer's Disease

Angela De Simone,^a Manuela Bartolini,^b Andrea Baschieri,^c Kim Y.P. Apperley,^d Huan Huan Chen,^a Melissa Guardigni,^a Serena Montanari,^a Tereza Kobrlova,^e Ondrej Soukup,^e Luca Valgimigli,^c Vincenza Andrisano,^a Jeffrey W. Keillor,^d Manuela Basso,^f Andrea Milelli^{a*}

^a Department for Life Quality Studies, *Alma Mater Studiorum*-University of Bologna, Corso d'Augusto 237, 47921 Rimini, Italy

^b Department of Pharmacy and Biotechnology, *Alma Mater Studiorum*-University of Bologna, Via Belmeloro 6, 40126 Bologna, Italy

^c Department of Chemistry "G. Ciamician", *Alma Mater Studiorum*-University of Bologna, Via S. Giacomo 11, 40126 Bologna, Italy

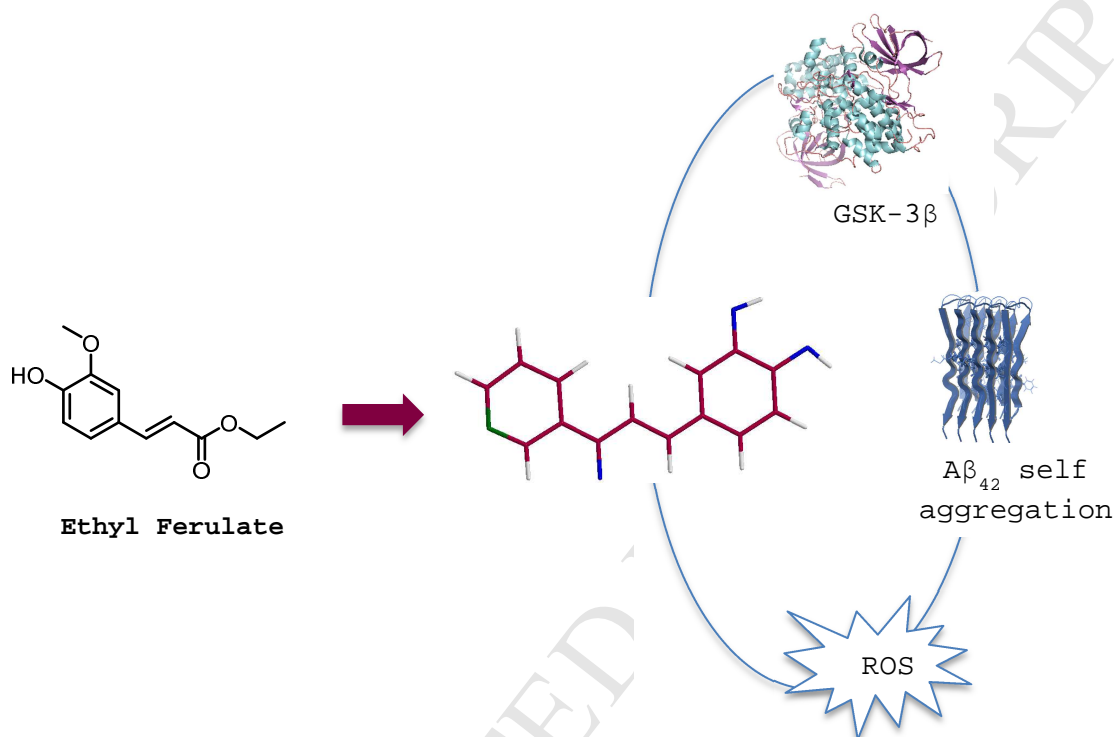
^d Department of Chemistry and Biomolecular Sciences, University of Ottawa, 10 Marie-Curie, Ottawa, ON, Canada K1N 6N5

^e Biomedical Research Center, University Hospital, Sokolska 581, 500 05 Hradec Kralove Czech Republic

^f Laboratory of Transcriptional Neurobiology, Centre for Integrative Biology, University of Trento, Via Sommarive 9, 38123 Trento, Italy

Corresponding Author. Dr. Andrea Milelli, Phone: Tel. +390541434610, Fax +390541434608. E-mail: andrea.milelli3@unibo.it.

Graphical abstract



Abstract

Alzheimer's disease (AD) is a multifactorial pathology that requires multifaceted agents able to address its peculiar nature. In recent years, a plethora of proteins and biochemical pathways has been proposed as possible targets to counteract neurotoxicity. Although the complex scenario is not completely elucidated, close relationships are emerging among some of these actors. In particular, increasing evidence has shown that aggregation of amyloid beta (A β), glycogen synthase kinase 3 β (GSK-3 β) and oxidative stress are strictly interconnected and their concomitant modulation may have a positive and synergic effect in contrasting AD-related impairments. We designed compound **3** which demonstrated the ability to inhibit both GSK-3 β ($IC_{50} = 24.36 \pm 0.01 \mu M$) and A β_{42} self-aggregation ($IC_{50} = 9.0 \pm 1.4 \mu M$), to chelate copper (II) and, in addition, to act as exceptionally strong radical scavenger ($k_{inh} = 3.2 \pm 0.5 \cdot 10^5 M^{-1}s^{-1}$) even in phosphate buffer at pH 7.4 ($k_{inh} = 3.2 \pm 0.5 \cdot 10^5 M^{-1}s^{-1}$). Importantly, compound **3** showed high-predicted blood-brain barrier

permeability, did not exert any significant cytotoxic effects in immature cortical neurons up to 50 μ M and showed neuroprotective properties at micromolar concentration against toxic insult induced by glutamate.

1. Introduction

Multifactorial diseases, such as cancer and neurological disorders, are driven by dysregulation of different but interconnected biochemical pathways. The complexity of these pathologies makes them hardly addressable by single-target molecules. In response, during the last two decades the scientific community has focused on a “multitarget drug design” approach, which may represent a major breakthrough in drug discovery.[1, 2] The cornerstone of this design strategy is the assumption that a multifactorial disease could be better contrasted by a chemical entity characterized by a similar complexity, called a MultiTarget Ligand (MTL). Indeed, the simultaneous modulation of multiple targets by a MTL should more significantly impact the course of disease progression.

One of the most active area of application of this strategy has been against the search for an effective treatment for Alzheimer’s disease (AD).[3] AD is a multifactorial and heterogeneous pathology characterized by the aberrant processing of two key players, namely amyloid- β peptide ($A\beta$), that leads to the formation and accumulation of senile plaques, characterized by aggregates of $A\beta$,[4] and tau-protein, whose hyperphosphorylation leads to the formation of neurofibrillary tangles (NFTs).[5] These aggregates, together with other pathogenic factors, such as oxidative stress, inflammation and excitotoxicity, trigger a cascade of interrelated pathways leading, ultimately, to neuronal cell death.[6]

Worldwide costs of AD are enormous (\$604 billion in 2010 [7]) and are estimated to further increase if no effective treatment will be found in the close future. Notwithstanding the urgent need for new therapies and in spite of massive efforts and investments, effective treatments are still unavailable.[8] Indeed, currently approved drugs are not effective in preventing, halting, or reversing AD the pathology, but only temporally ameliorating cognitive impairment by enhancing the cholinergic tone (acetylcholinesterase inhibitors-AChEIs) or counteracting the excitotoxicity exerted by glutamate (antagonist at the NMDA receptor) in the brain of AD patients. A survey of the drug candidates currently in clinical trials for AD [9] shows that several approaches addressing all critical pathological players in AD, i.e., amyloid- and tau-related toxicity, neuroinflammation, oxidative stress and neurodegeneration, are under investigation, without a clear higher beneficial advantage of one approach over the other.

The majority of the MTL strategies so far investigated have relied on coupling the scaffold of known AChEIs, such as tacrine, with a second fragment displaying additional biological activities, such as inhibition of A β aggregation or A β formation, scavenging activity towards reactive oxygen species (ROS), metal chelating properties and neuroprotection activity.[10-12]

~~Recently, in the search for more effective compounds, recently, new MTLs based on non-AChEI scaffolds have been proposed.~~ Bolognesi and co-workers have reported a new series of MTLs based on the triazinone scaffold as dual β -secretase (BACE-1)/glycogen synthase kinase 3 β (GSK-3 β) inhibitors.[13, 14] These agents inhibit enzymes that belong to the two main toxic pathways of AD, i.e., A β and tau-protein pathways, and display promising neuroprotective and neurogenic activities. These results further highlight the benefit of simultaneously targeting distinct points of the neurotoxic cascades.

BACE-1 is an aspartyl protease that is overexpressed in the brain of AD patients and cleaves the amyloid precursor protein (APP) leading, ultimately, to the formation and accumulation of A β peptide.[15] Therefore, treatments with BACE-1 inhibitors are envisioned as long-term therapy to limit A β production after removing existing amyloid deposits. On the other hand, GSK-3 β is responsible for tau hyperphosphorylation which triggers the formation of NFTs. [16] Furthermore, GSK-3 β has been suggested as a possible link between A β and tau. [17]

Several BACE-1 inhibitors are currently in different stages of clinical development.[9] However, therapeutic tuning of BACE-1 activity is a challenging task as demonstrated by the recent failure of verubecestat.[18] The complexity of such approach arises from the fact that APP is not the only physiological target of BACE-1 and it plays key roles in the myelination of neurons, in learning, memory, and in synaptic plasticity. [19] Furthermore, inhibition of BACE-2, a close homologous enzyme of BACE-1, is responsible for side effects in pancreas, skin and brain.[20]

Other than reducing A β generation through BACE-1 inhibition, neurotoxicity induced by A β aggregates can be counteracted by other approaches, such as increasing A β clearance, preventing its aggregation or interfering with the boosting effect on A β toxicity exerted by the dyshomeostasis of biometals in the brain. [21] Indeed, although the debate on the role of amyloid in the onset and progression of AD is still open, drug candidates directed toward A β have shown to be promising and have reached the last phases of clinical trials (fourteen drug candidates directed towards A β were in phase III clinical trials in June 2016).[9] Among these, aducanumab (Biogen), a human recombinant monoclonal antibody that selectively targets A β aggregates,[22] was granted Fast Track designation by the U.S. Food and Drug Administration (FDA) in 2016, underlining the

expected positive outcome from such an approach. These findings have renewed the interest of the scientific community for the amyloid hypothesis.[23]

~~Finally, several antioxidants with a multitarget mechanisms of action are currently investigated in clinical trials.[9] Indeed, it is well known that neurodegeneration processes in the central nervous system (CNS) are often initiated or enhanced by oxidative stress and that a critical link exists, since it promotes A β toxicity, and *vice versa*, and triggers the amyloidogenic pathway. Furthermore, oxidative stress was reported to affect the tau protein phosphorylation status and significantly increase GSK-3 β activity. Supporting these findings, the antioxidant compound melatonin was shown to decrease GSK-3 β activity and tau hyperphosphorylation *in vitro* and *in vivo*.~~

Finally, compelling evidence has shown that neurodegenerative processes in the central nervous system (CNS) are often initiated or enhanced by an increased oxidative stress, which precedes the appearance of the hallmarks of the disease.[24-26] Furthermore, oxidative stress was reported to affect tau protein phosphorylation [27] and to significantly increase GSK-3 β activity.[28, 29] Supporting these findings, the antioxidant compound melatonin was shown to decrease GSK-3 β activity and tau hyperphosphorylation *in vitro* and *in vivo*. [30] These observations laid down the basis for the clinical investigation of several antioxidants with a multitarget mechanisms of action.[9]

On these premises, the aim of the present investigation is the discovery of a pharmacological tool able to block the neurodegenerative cascade by operating at critical points of the two major pathogenic mechanisms, i.e., targeting both A β self-aggregation and GSK-3 β activity, and to disrupt the vicious circle involving oxidative stress, A β toxicity and tau hyperphosphorylation (Figure 1).

To this purpose, we focused our attention on ferulic acid ethyl ester (ethyl-4-hydroxy-3-methoxycinnamic acid), a natural antioxidant which exerts protective effects on neurons against A β -induced toxicity by modulating the oxidative stress both directly and indirectly through the induction of protective genes.[31] Furthermore, the chemical structure of ferulic acid ethyl ester also offered the possibility to be easily modified in order to broaden its biological activity. Indeed, the *trans*-cinnamoyl scaffold represents a privileged structure and plenty of compounds based on this structure have been evaluated against a plethora of biological targets.[32-34]

Five *trans*-cinnamoyl derivatives (**1-5**) were designed to i) act as antioxidants thanks to the substituted aromatic moiety deriving from natural products, such as ferulic and caffeic acids and ethyl ferulate, ii) interact with GSK-3 β through the α,β -unsaturated system[35] and iii) counteract A β_{42} self-aggregation thanks to the substituted aromatic moiety and the presence of an extended planar conjugate system.[36] The introduction of a 3-pyridinyl 3-pyridyl ring was envisaged to

have a double role. Indeed, its extended conjugate system could allow a better interaction with A β ₄₂ growing fibrils and establish additional interactions with GSK-3 β .

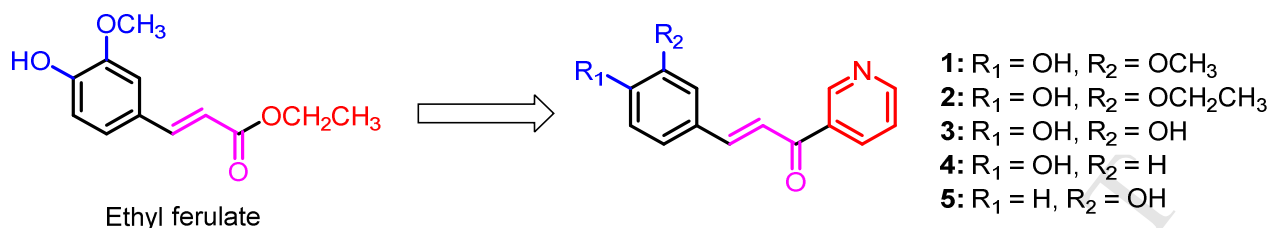


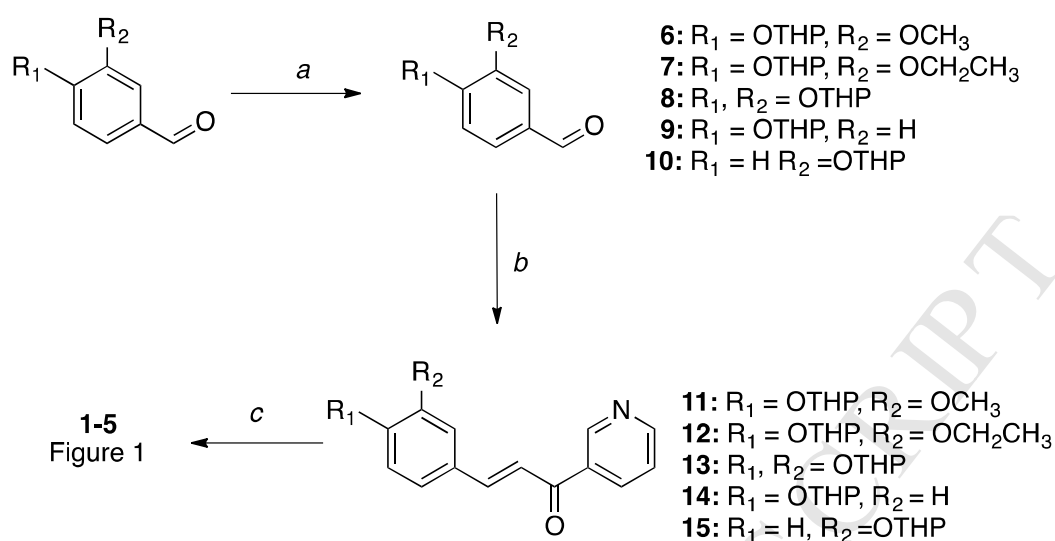
Figure 1. Design strategy leading to derivatives **1-5**.

To confirm the multifunctional activity profile envisaged for the designed compounds, derivatives **1-5** were evaluated for their ability to inhibit GSK-3 β and A β ₄₂ self-aggregation and to counteract reactive oxygen radical (ROS) formation.

Furthermore, for the most interesting compound, the ability to chelate copper, a biometal involved in AD neurotoxicity, was evaluated together with the neuroprotective activity against glutamate-induced toxicity in cortical neurons. Furthermore, due to the structural similarity to well-known inhibitors of transglutaminase 2 (Tg2)[37] and the role of this enzyme in AD pathogenesis, the inhibitory activity towards Tg2 was also determined. Indeed, Tg2 is an enzyme that catalyzes the post translational modifications of proteins whose expression and activities are increased in brain areas affected by AD.[38] Tg2 was suggested to be able to initiate A β aggregation and induce the formation of high-molecular weight tau aggregates. Therefore, inhibition of Tg2 might implement the overall beneficial activity of a new therapeutic for AD treatment. Lastly, since activity should be exerted in the CNS, for representative compounds the prediction of the blood-brain barrier (BBB) permeability was investigated by BBB-PAMPA assay.

2. Chemistry

The synthesis of the target compounds is reported in Scheme 1. Briefly, the hydroxyl group(s) of the appropriate aldehydes were protected as tetrahydropyranyl ethers and the resulting compounds (**6-10**) were then subjected to a classic base-catalyzed aldol reaction with 3-acetylpyridine, leading to α,β -unsaturated ketones **11-15**. Acidic hydrolysis of the aldol adducts **11-15** led to the corresponding final compounds **1-5**.



Scheme 1. a) 3,4-Dihydro-2H-pyran, pyridinium *p*-toluenesulfonate, dichloromethane, rt, 12 h; b) 3-acetylpyridine, 2.5 M aq. NaOH, rt, 12 h; 38-60 yields; c) *p*-Toluenesulfonic acid, methanol, rt, 12 h; 41-72 yields.

2. Results and Discussion

2.1 Inhibitory activity toward GSK-3 β

Based on the expected activity profile, compounds **1-5** were evaluated for their ability to inhibit GSK-3 β , in comparison with ethyl ferulate, using a luminescence assay. [39] Compounds were first screened at a single concentration, namely 50 μ M, and for the most active derivative the IC₅₀ value was measured. As reported in Table 1, although the introduction of a pyridinyl 3-pyridyl group induced an increase in the inhibitory activity compared to ethyl ferulate, all compounds, with the exception of **3**, show poor inhibitory potency with values ranging from 25.2 to 43.5% ([I] = 50 μ M). Surprisingly, Compound **3**, characterized by a 2,3-dihydroxy substitution on the aromatic ring, turned out to be a good inhibitor of GSK-3 β with an IC₅₀ value of 24.36 \pm 0.01 μ M. The structural requirements for a good inhibition seem to be quite strict. Indeed, the substitution of an hydroxyl group with a methoxy or ethoxy group, as in compounds **1** and **2**, or the presence of a single hydroxy group on the aromatic ring, as in **4** and **5**, led to compounds with a weak inhibitory activity.

The inhibitory potency of compound **3** lies in the micromolar range, which is in line with the activity of other GSK-3 β -based multipotent compounds.[14] Evidence from *in vivo* studies suggests

that inhibition at micromolar concentration would be adequate to produce therapeutic effects in the brain without affecting GSK-3 β activity in peripheral tissues.[40]

2.2 Inhibition of A β ₄₂ self-aggregation

The anti-aggregating activity toward A β ₄₂ of compounds **1-5** was determined by a thioflavin (ThT)-based fluorometric assay.[41] The ThT-based assay is among the most widely used methods to screen small molecules as inhibitors of amyloid aggregation and fibrillization. In such an assay, emission at 490 nm is assumed to be directly proportional to the quantity of formed amyloid fibrils. To exclude any positive or negative interference in the fluorescence signal due to quenching or displacement phenomena, fluorescence emission intensities of preformed A β ₄₂ fibrils (in a 1.5- μ M ThT solution) in the absence and presence of inhibitor were compared. No significant interference was observed under the experimental conditions (Δ IF \leq 10% for the highest tested concentration). Similarly to what was observed for the inhibition of GSK-3 β , all the compounds, with the exception of compound **3**, turned out to be poor inhibitors with inhibition ranging between 5.8 and 21.5% when tested at a 1:1 ratio with A β ₄₂. Differently to the other compounds of the series, compound **3** proved to be a potent inhibitor of A β ₄₂ self-aggregation with an IC₅₀ of $9.0 \pm 1.4 \mu\text{M}$. Therefore, the substitution pattern of the aromatic ring strongly influenced the ability to interfere with A β ₄₂ aggregation, since all modification of the 3,4-dihydroxyl-derivative proved to be ineffective. The good anti-aggregating activity of **3** is in agreement with the well-known ability of polyphenols to modulate A β aggregation.[42] Furthermore, these findings are partially in line with the report from Reinke et al. concerning a structure-activity relationships (SAR) study on curcumin derivatives.[36] Indeed, the activity profile of compounds **1-5** clearly stated that the nature of the substitution of the aryl group is more critical than the size of the planar aromatic system for a productive interaction with A β . [36] Compound **3** showed a higher inhibitory potency than that of the parent compounds ferulic acid, 3-hydroxycinnamic acid (IC₅₀ > 100 μM for both compounds)[36] and caffeic acid (32.3 ± 3.7 % inhibition at 20 μM).[43] For the sake of completeness it must be pointed out the different ionization status of the latter compounds in comparison with derivatives **1-5** in the experiment conditions that might influence the inhibitory activity.

On the basis of data available in the literature, compound **3** can be ranked as a strong inhibitor of A β ₄₂ self-aggregation, with potency very close to that of the well-known multipotent compound bis(7)-tacrine (IC₅₀ = $8.4 \pm 1.4 \mu\text{M}$)[44] and slightly more potent than catechol derivative recently proposed by Simoni *et al.* [(*S*)-allyl (*E*)-3-(3,4-dihydroxyphenyl)prop-2-enethioate, IC₅₀ = $12.5 \pm 0.9 \mu\text{M}$).[45]

Table 1. Inhibition of GSK-3 β , A β ₄₂ self-aggregation, Tg2 and antioxidant activity.

Compounds	GSK-3 β ^a		A β ₄₂ self-aggregation		antioxidant activity in PhCl (T = 30 °C)		Tg2 IC ₅₀ (μ M) \pm SEM
	% inhibition \pm SEM ^b	IC ₅₀ (μ M) \pm SEM	% inhibition \pm SEM ^c	IC ₅₀ (μ M) \pm SEM	$k_{inh}/M^{-1}s^{-1d}$	n^e	
1	37.18 \pm 0.10	n.d.	17.5 \pm 1.7	n.d.	7.1 \pm 0.2 \cdot 10 ³	2.1 \pm 0.1	688 \pm 105
2	39.55 \pm 0.60	n.d.	18.8 \pm 0.5	n.d.	6.1 \pm 0.3 \cdot 10 ³	2.1 \pm 0.1	484 \pm 15
3	100	24.36 \pm 0.01	91.5 \pm 0.5	9.0 \pm 1.4	6.8 \pm 0.5 \cdot 10 ⁵ 3.2 \pm 0.5 \cdot 10 ^{5f}	2.6 \pm 0.3 4.5 \pm 0.2	1001 \pm 35
4	25.18 \pm 0.01	n.d.	21.5 \pm 5.8	n.d.	5.7 \pm 0.3 \cdot 10 ³	2.0 \pm 0.2	> 2000
5	43.55 \pm 0.01	n.d.	5.8 \pm 5.3	n.d.	1.5 \pm 0.2 \cdot 10 ³	1.9 \pm 0.2	266 \pm 22
Ethyl ferulate	21.38 \pm 0.06	n.d.	n.d.	n.d.	4.6 \pm 0.2 \cdot 10 ³	2	n.d.

^a Values are the mean of two independent measurements, each performed in duplicate. ^b Assay performed in presence of 50 μ M inhibitor. ^c Assays were carried out in the presence of 50 μ M inhibitor and 50 μ M A β ₄₂. ^d Rate constant for reaction with alkylperoxyl radicals. ^e Stoichiometric factor = number of peroxyl radicals trapped by one molecule of antioxidant. ^f Experiment performed in 0.1M aqueous phosphate buffer (pH = 7.4), THF 3.1M, [AAPH] 25 mM, T = 30°C. nd stands for not determined; SEM stands for standard error of the mean.

2.3 Copper chelating properties

Strong relationships exist between A β and biometals, and changes in the transition metals, zinc, copper and iron, have shown to impact the molecular mechanisms of the disease.[46] High concentration of metals have been found in amyloid plaques.[47] It is also reported that copper is able to contribute to the formation of neurotoxic ROS[48] and accelerate the formation of A β oligomers.[49] Thus, agents targeting such metals have been proposed as an alternative strategy for the treatment of AD[46] and extensive preclinical and clinical data underlie the rationale of such approach.

Based on its interesting activity profile towards GSK-3 β and A β ₄₂, compound **3** was selected for further characterization. In particular, the chemical structure of compound **3** makes it a potential chelating agent. Thus, it was investigated for its ability to complex Cu²⁺ ions by means of UV-vis differential spectroscopy. The UV-vis spectrum of compound **3** in methanol showed band maxima at 244 nm ($\epsilon = 10136 M^{-1} cm^{-1}$), 266 nm ($\epsilon = 11013 M^{-1} cm^{-1}$) and 374 nm ($\epsilon = 19087 M^{-1} cm^{-1}$) as detailed in the Supporting Information. Upon addition of CuCl₂, absorbance at those wavelengths was reduced and a new band appeared with maximum at 460 nm, which increased with the metal concentration (Figure 2). Spectral changes were most accurately monitored from the differential spectra, which were obtained by numerically subtracting the spectra of ligand and metal (at the corresponding molar concentration) from the spectrum of the mixture (Figure 2B). Since they were dependent on the relative concentration of metal/ligand and showed saturability, it was possible to

use UV–Vis spectroscopy to determine the stoichiometry of complex formation. When increasing concentrations of CuCl_2 were added to a $7.5 \mu\text{M}$ solution of compound **3** (in methanol) the signal at 460 nm , attributable to complex formation, progressively increased up to the addition of 0.5 equivalents of Cu^{2+} . No further increase of the absorbance was observed from 0.5 to 2 equivalents of Cu^{2+} . This spectral variation paired a corresponding decrease in the absorbance at 374 nm (Figure 2C), indicating a preferred stoichiometry for the **3**/ Cu^{2+} complex of $2:1$, as expected for Cu^{2+} complexes with catechol.[50] Analysis of Figure 2C indicates that, even at low micromolar concentrations, Cu^{2+} ions are quantitatively chelated by compound **3**. While this very high affinity prevented a quantitative assessment of the binding constant, it confirmed the expected relevance of this interaction under biomimetic settings.

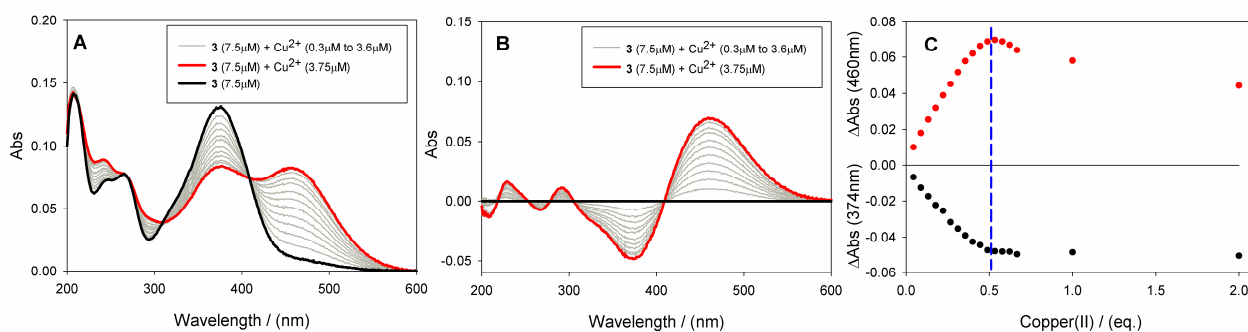


Figure 2. (A) UV–Vis (200–600 nm) absorption spectra of **3** ($7.5 \mu\text{M}$) in methanol after addition of ascending amounts of CuCl_2 (0.30 – 3 – $3.75 \mu\text{M}$); (B) differential spectra of **3**- Cu^{2+} complex formation obtained by numerical subtraction of CuCl_2 and **3** spectra from the above spectra, at the corresponding concentrations, and (C) plot of the differential absorbance at 460 and 374 nm as a function of the equivalents of Cu^{2+} added to the solution.

In the light of the confirmed chelating properties, compound **5** might also prevent biometal induced-amyloid aggregation and attenuate the neurotoxic cascade triggered by the amyloid-metal complex. Because of the potentially relevant therapeutic implications these aspects deserve further investigation.

2.4 Antioxidant activity

Because of the strict connection between $\text{A}\beta$, tau, biometals and oxidative stress, compounds **1-5** were also evaluated for their ability to counteract ROS. The antioxidant activity was investigated by measuring the kinetics of oxygen consumption during the controlled inhibited autoxidation of a standard substrate, which is currently the best-established method to obtain mechanistic insights and

accurate quantitative data to draw SARs[51]. With this method, in the absence of antioxidants, oxygen consumption during the autoxidation (forcibly initiated at a rate R_i by an azo-compound) is constant. Addition of micromolar concentrations of the test antioxidant would produce either a neat inhibited period (until the antioxidant is consumed) or a decrease in the slope of oxygen-uptake plots, whose analysis (*e.g.* by eqs. 1-2) affords the absolute rate constant k_{inh} for the reaction between the antioxidant and the oxidative chain-carrying peroxy radicals, and the so-called stoichiometric factor, n , i.e. the number of peroxy radicals trapped by one molecule of antioxidant. Representative plots recorded for compounds **1-5** are shown in Figure 3. Because of similar structural motif and electronic properties, ethyl ferulate, a representative structure among polyphenolic antioxidants,[52] was investigated for comparison.

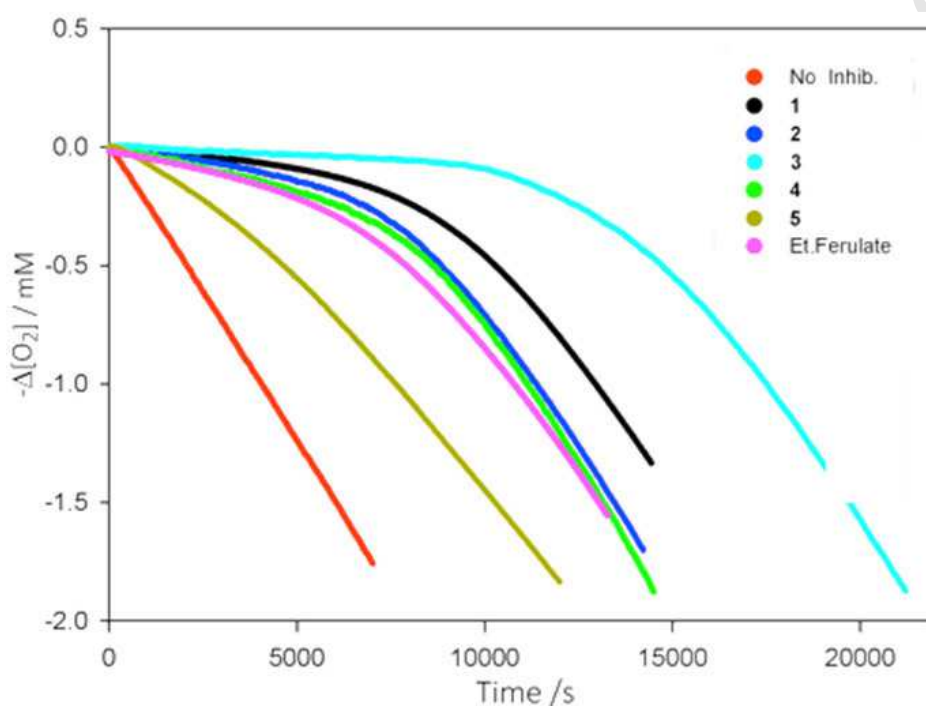


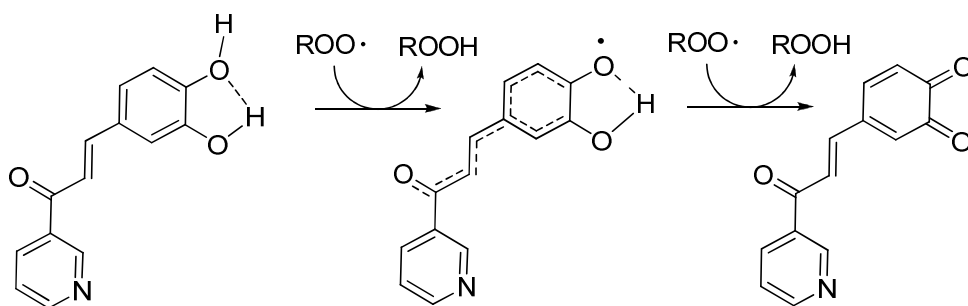
Figure 3. Oxygen consumption during the autoxidation of cumene (3.6 M) initiated by AIBN (0.05 M) in PhCl at 30°C without inhibitors (red) or in the presence of compounds **1-5** and reference compound ethyl ferulate (24 μ M).

All investigated compounds were able to effectively inhibit the autoxidation of cumene in apolar organic solution (PhCl), each trapping 2 peroxy radicals, as expected for a typical phenolic antioxidant, as summarized in Table 1. Rate constants nicely reflected the substitution pattern in the phenolic ring. Compound **5**, bearing only the electron withdrawing (EW) 3-pyridyl-oxopropenyl group in the *meta* position, showed the lowest reactivity, while isomeric compound **4** had almost 4-

fold enhanced reactivity due to stabilization of the intermediate product phenoxyl radical by delocalization of the unpaired electron in the oxopropenyl chain. Indeed, while EW substituents are known to increase the O-H bond dissociation enthalpy (BDE) of phenols, thereby decreasing their reactivity, extension of the conjugated π -systems works in the opposite direction.[53] The compensating behavior of the two factors is clearly visible upon considering the reactivity of reference ethyl ferulate, which is identical to that previously measured for guaiacol (2-methoxyphenol, $k_{\text{inh}} = 4.7 \times 10^5 \text{ M}^{-1} \text{ s}^{-1}$ [52]). In ethyl ferulate, as well as in compounds **1** and **2**, reactivity is also affected by the presence of the *ortho*-alkoxy substituent, which, again, acts by a combination of (partially) compensating effects: the net electron donating (ED) character of the RO substituent in *ortho* position would lower the phenolic O-H BDE, but it is almost compensated by the introduction of an intramolecular H-bond and an increase in steric hindrance around the reactive site, which impairs the reactivity.[54, 55] As a result, compound **1** was approximately 20% more effective than compound **4**, while the advantage was lost with compound **2** due to higher steric hindrance.

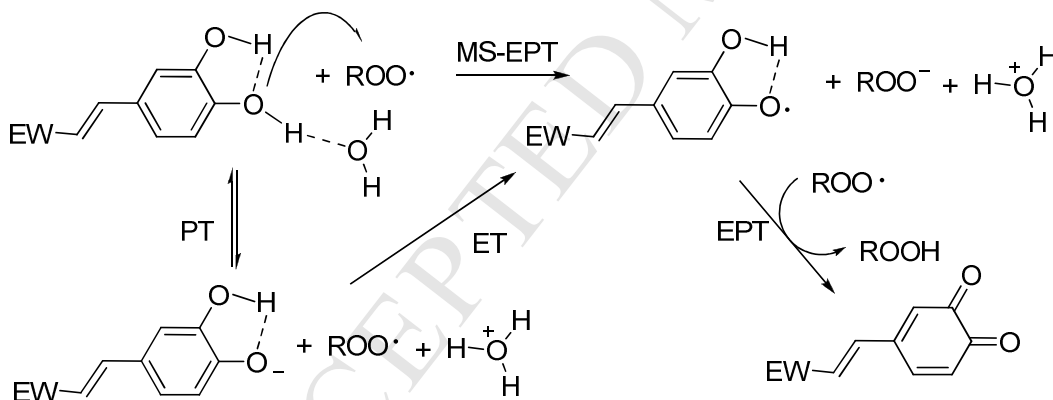
The EW 3-pyridyl moiety has been extensively investigated in recent years to afford more stable, less toxic and more effective antioxidants.[53] Its contribution is visible in compounds **1** and **2**, which were respectively 33% and 54% more effective than reference ethyl ferulate in trapping peroxy radicals. Most interesting, however, was the contribution of the chosen structural motif 3-pyridyl-oxopropenyl group in the antioxidant behaviour of compound **3**, whose reactivity surpassed any other investigated compound by two orders of magnitude, being nearly 150-fold more effective than reference ethyl ferulate. Such reactivity may be due to a combination of factors, summarized in Scheme 2. The catechol ring is a privileged structure for antioxidant activity among phenols, since the intramolecular H-bonding between the neighboring OH groups impairs the reactivity of one (acting as H-bond donor) while it greatly enhances the reactivity of the other OH (acting as H-bond acceptor), due to the strengthening of the H-bond as the reaction with peroxy radicals proceeds with the formation of the corresponding H-bonded semiquinone radical.[53]

Delocalization of the unpaired electron in the 3-pyridyloxopropenyl moiety further stabilizes the radical, which makes compound **3** over 2-fold more reactive than structurally related caffeic acid ($k_{\text{inh}} = 2.9 \times 10^5 \text{ M}^{-1} \text{ s}^{-1}$),[56] surpassing the antioxidant performance of quercetin ($k_{\text{inh}} = 5 \times 10^5 \text{ M}^{-1} \text{ s}^{-1}$) and matching that of 5-hydroxytyrosol, the well-established antioxidant found in olive ($k_{\text{inh}} = 8 \times 10^5$), measured under identical conditions.[57]



Scheme 2. Reaction of compound **3** with peroxy radicals in apolar organic solvents.

Since compound **3** showed the highest antioxidant activity among tested compounds, its reactivity was further investigated in aqueous phosphate buffer solution, using tetrahydrofuran as a model oxidation substrate.[58] At variance with other phenolic and polyphenolic antioxidants that experience major impairment of their antioxidant performance in water due to H-bonding to the solvent– which typically reduces the k_{inh} of up to two orders of magnitude - compound **3** maintained exceptionally high reactivity with k_{inh} of $3.2 \times 10^5 \text{ M}^{-1} \text{ s}^{-1}$. By comparison with previous investigations with unsubstituted catechol and other phenols, a mechanistic explanation can be suggested as depicted in Scheme 3.

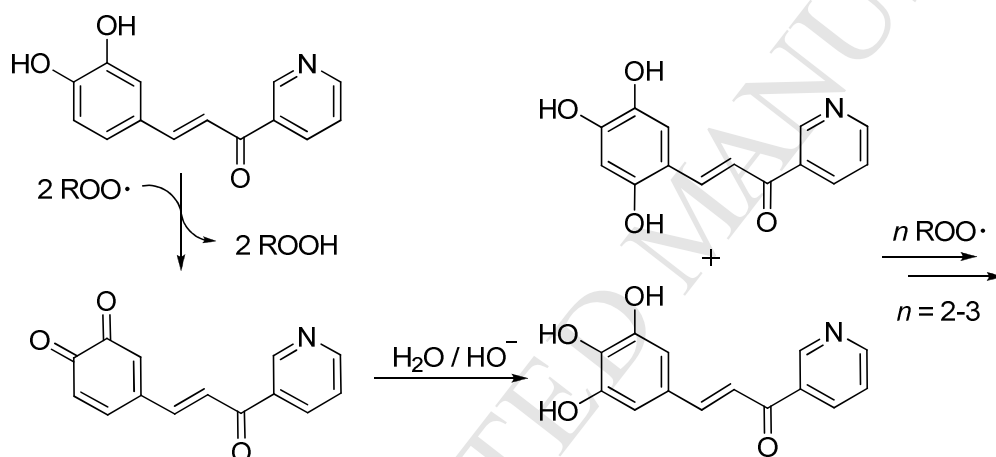


Scheme 3. Reaction mechanism of compound **3** with peroxy radicals in water.

The EW character of the side chain increases the acidity of the catechol to the point where it causes a shift in the reaction mechanism, from a formal H-atom transfer, *i.e.* the concerted electron-proton transfer (EPT) to the peroxy radical, to a dual mechanism in which the proton is transferred to the solvent (or to the buffer) and one electron is transferred to the peroxy radical. The duality of the mechanism is related to the relative timing of the PT and ET events that can either occur stepwise

(PT-ET mechanism) or concertedly but to different acceptors in a so-called, multi-site EPT (PT to the solvent and ET to the peroxy radical). With both mechanistic possibilities, H-bonding to the solvent is not expected to slow down the reaction to any major extent,[58] as observed experimentally.

Another aspect of the antioxidant behaviour of compound **3** that merits discussion is its exceptionally high stoichiometric factor in water ($n = 4.5$ as opposed to typical $n = 2$). Again this is attributed to the electronic properties of the side chain enabling rapid Michael-type nucleophilic addition of water to the ortho-quinone formed upon trapping the first two peroxy radicals. Enolization to a polyhydroxylated aromatic ring allows subsequent rapid reaction with additional peroxy radicals, as illustrated in Scheme 4.



Scheme 4. Proposed mechanism for extended stoichiometry of antioxidant activity of compound **3** in water.

Beside expressing antioxidant behaviour, potentially, reducing antioxidants (including ascorbate) could also express a paradoxical pro-oxidant behaviour under some settings; specifically, as in the case of autoxidations initiated by Fenton-type chemistry in the presence of transition metal ions. [51] This would be linked to their ability to reduce (i.e. recycle) metals from their higher oxidation state (e.g. Cu^{2+} to Cu^+), making them available for reaction with peroxides. [51] To investigate this possibility for compound **3**, we performed a series of experiments in water where autoxidation was initiated by the redox couple $\text{Cu}^+/\text{Cu}^{2+}$ in the presence of hydrogen peroxide. In no case we observed a pro-oxidant behaviour for compound **3**. A representative experiment is shown in Figure S3. Clearly, this does not exclude that compound **3** can express pro-oxidant chemistry to some

extent; however this is overwhelmed by the antioxidant behaviour, that prevails under any tested experimental settings.

2.5 Inhibitory activity toward Transglutaminase 2

Some cinnamoyl-pyridines have been reported as Tg2 inhibitors.[37] Tg2 is an enzyme that catalyzes the post translational modifications of proteins whose expression and activities are increased in brain areas affected by AD.[38] In particular, Tg2 is observed in senile plaques[59]. Furthermore, NFT[60], A β and tau, either in phosphorylated and non-phosphorylated forms, are substrates of Tg2-catalyzed modifications.[61, 62] Experimental evidence suggests that Tg2 may initiate the aggregation process of A β and induces the formation of high-molecular weight tau aggregates, which are more resistant to enzymatic degradation. Furthermore, Tg2 inhibitors were shown to counteract A β -induced toxicity in the SH-SY5Y cell line.[63] Therefore, compounds **1-5** were evaluated for their ability to inhibit Tg2. Results in Table 1 show that these compounds act as low to moderate inhibitors of Tg2, depending on the substitution pattern of the hydroxyl/alkoxy groups on the aromatic ring. Compound **5** was found to be the most potent Tg2 inhibitor within this series, although its potency is roughly an order of magnitude lower than that reported for the inhibition of guinea pig liver TGase by similar azachalcones.[37]

2.6 Cell toxicity and neuroprotection

Glutamate is a major excitatory neurotransmitter in mammalian CNS. Excessive glutamate releasing overactivates its receptors causing calcium dyshomeostasis, increasing the production of ROS and initiating a cascade of intracellular events leading to neuronal degeneration. Based on its promising *in vitro* profile, compound **3** was investigated for its protective effect on neurons undergoing oxidative stress. In particular, immature cortical neurons were treated at day *in vitro* 1 (DIV1) with glutamate, to block the X_{ct} transporter and reduce the intracellular levels of glutathione, and with increasing concentrations of compound **3**. [64, 65] Viability was assessed by MTT assay after 24 hours in three different neuronal preparations. Interestingly, compound **3** did not show any toxic effects in this cell line up to 50 μ M, resulting safe at concentrations at which it exerts its biological activity. Furthermore, as shown in Figure 5, compound **3** was able to block neuronal death induced by glutamate (5 mM) already at the concentration of 12.5 μ M.

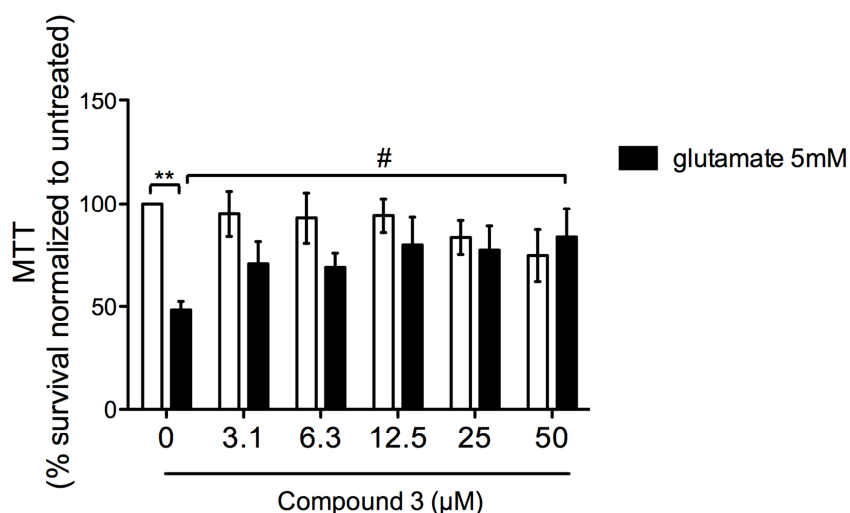


Figure 5. Compound **3** protects cortical neurons from oxidative-stress mediated cell death. Immature neurons (DIV1) were treated with increasing concentrations of compound **3** in presence (black bars) and in absence (white bars) of glutamate, able at high concentration (5mM) to deplete neurons of their major antioxidant, glutathione, and induce oxidative stress. Compound **3** blocks glutamate toxicity already at low μM concentrations with statistical significance at $50\mu\text{M}$. The data were analyzed with two-way ANOVA and Bonferroni's *post hoc* test; $**p<0.01$ and it is referred to the significant difference between untreated and glutamate treated neurons ($0\mu\text{M}$). $\#p<0.05$ and it compared the neuronal viability in glutamate-treated neurons in the absence of compound **3** with glutamate-treated neurons in the presence of compound **3** ($50\mu\text{M}$).

2.7 Blood–brain barrier penetration

Penetration across the BBB is an essential property for compounds targeting the CNS. Thus, in order to predict passive BBB permeability of novel compounds a modification of the parallel artificial membrane permeability assay (BBB-PAMPA) was used.[66, 67] PAMPA assay is widely used as pre-screening tool in early drug discovery to investigate drug permeation through biological barriers. Data obtained for compounds **1**, **3** and **5** were correlated to standard drugs among which the anti-AD drugs donepezil, rivastigmine and tacrine. For such reference drugs the Permeability (P_e) values were previously determined using PAMPA assay in the same experimental conditions and their CNS availability is known.[66, 68] Prediction of BBB penetration of compounds **1**, **3**, and **5** is summarized in Table 2. Compounds **1**, **3** and **5** showed P_e values similar to those determined for the reference AD drugs and have high probability to cross the BBB via passive diffusion [P_e ($10^{-6} \text{ cm s}^{-1}$) > 4.0].

Table 2: Prediction of blood-brain barrier penetration of drugs expressed as $Pe \pm SEM$ (n=2).

BBB penetration estimation		
Compound	$Pe \pm SEM$ ($\times 10^{-6} \text{ cm s}^{-1}$)	CNS (+/-)
1	9.9 ± 0.4	CNS (+)
3	5.5 ± 0.3	CNS (+)
5	6.5 ± 0.4	CNS (+)
Donepezil	7.3 ± 0.9	CNS (+)
Rivastigmine	6.6 ± 0.5	CNS (+)
Tacrine	5.3 ± 0.2	CNS (+)
Testosterone	11.3 ± 1.6	CNS (+)
Chlorpromazine	5.6 ± 0.6	CNS (+)
Hydrocortisone	2.9 ± 0.1	CNS (+/-)
Piroxicam	2.2 ± 0.1	CNS (+/-)
Theophylline	1.1 ± 0.2	CNS (-)
Atenolol	1.0 ± 0.4	CNS (-)

CNS (+) (high BBB permeation predicted); Pe ($10^{-6} \text{ cm s}^{-1}$) > 4.0 ; CNS (-) (low BBB permeation predicted); Pe ($10^{-6} \text{ cm s}^{-1}$) < 2.0 ; CNS (+/-) (BBB permeation uncertain); Pe ($10^{-6} \text{ cm s}^{-1}$) from 4.0 to 2.0.

3. Conclusions

AD is a multifactorial disease whose development depends on the dysregulation of several interconnected biochemical pathways. For instance, strict connections exist between the main neurotoxic pathways involved in AD, namely $A\beta$ and tau, and oxidative stress is emerging as a key modulator of the toxicity induced by both proteins. Indeed, oxidative stress promotes $A\beta$ toxicity and increases GSK-3 β mediated tau hyperphosphorylation. Finally, biometals accumulation in the brain may increase amyloid-related toxicity. Therefore, the development of a single molecule able to contrast both $A\beta$ and tau-induced toxicity, and break the vicious circle induced by oxidative stress, could represent a promising strategy in the design of effective anti-AD agents. As a proof of concept of the feasibility of generating a single molecule able to exert such a multiple action, we reported the design and preliminary characterization of compound **3** which may be able to contrast AD neurotoxicity by acting at different levels of the neurotoxic cascade. In particular, experimental outcomes clearly indicate that compound **3** is able to modulate GSK-3 β and $A\beta_{42}$ self-induced aggregation. Furthermore, compound **3** acts as copper chelator and, more interestingly, exerts a very high ROS scavenging activity in aqueous medium. A detailed investigation of the scavenging properties of related compounds allowed clarifying the exceptionally high scavenging activity.

Considering the transversal role of oxidative stress, which seems to be the “fil rouge” of the whole AD pathology, being cited as causing or resulting pathological hallmark in all hypothesis for AD pathogenesis, the high antioxidant activity combined with the inhibitory actions toward GSK-3 β and A β ₄₂ makes **3** a very promising compound.

Finally, compound **3** showed to be safe when tested in immature cortical neurons up to 50 μ M and was able to protect these neurons from toxic stimuli induced by glutamate and was predicted to have a good BBB permeability. In light of these considerations, compound **3** could be considered a promising tool to investigate AD pathogenesis and may be worth for further development in the search for an effective anti-AD drug candidate.

4. Experimental Section

4.1 Chemistry

Uncorrected melting point was taken in glass capillary tubes on a Buchi SMP-20 apparatus. The elemental analysis was performed with Perkin Elmer elemental analyzer 2400 CHNESI. MS spectra were recorded on Perkin Elmer 297 and Waters ZQ 4000 and Micromass Q-TOF Ultima Global. ¹H NMR and ¹³C NMR were recorded on Varian VRX 200 and 400 instruments. Chemical shifts are reported in parts per million (ppm) relative to peak of tetramethylsilane (TMS) and spin multiplicities are given as s (singlet), br s (broad singlet), d (doublet), dd (doublet of doublets) t (triplet), td (doublet of triplets), q (quartet) or m (multiplet). Chromatographic separations were performed on silica gel columns by flash (Kieselgel 40, 0.040 e 0.063 mm, Merck) column chromatography. Reactions were followed by thin layer chromatography (TLC) on Merck (0.25 mm) glass-packed pre-coated silica gel plates (60 F254) and then visualized in an iodine chamber or with a UV lamp. Reagents and solvents have been purchased by Sigma Aldrich and used as received unless otherwise reported. THF was distilled and stored under argon at 5 °C; the content in hydroperoxides was determined periodically by spectrophotometry at 262 nm in isopropanol upon reaction with triphenylphosphine, and found <50 ppm (μ g g⁻¹). Cumene and styrene were purified by double percolation through silica and activated alumina columns before use. AIBN was recrystallized from methanol and stored at -18 °C. Phosphate buffer solution (pH 7.4) were prepared as previously described, were mixed with the desired amount of THF (3:1 by volume) after having adjusted the pH to the desired value.[69]

4.1.1 General procedure for the synthesis of compounds 1-5

To the appropriate protected aldol-adduct **11-15** in methanol, ~~para-toluenesulfonic acid~~ para-toluenesulfonic acid (cat.) was added and the resulting mixture was stirred at room temperature overnight. The solvent was removed under vacuum and the obtained residue was purified through flash chromatography leading to the unprotected final products **1-5**.

4.1.1.1 (*E*)-3-(4-hydroxy-3-methoxyphenyl)-1-(pyridin-3-yl)prop-2-en-1-one (**1**)

Compound **1** was obtained from compound **11**; eluting mixture dichloromethane / methanol (9.8:0.2); yellow solid; 61% yield; mp = 181-183 °C; ¹H-NMR (CDCl₃, 400 MHz) δ 3.99 (s, 3H), 6.98 (d, 1H, J = 8.0 Hz), 7.15 (d, 1H, J = 2), 7.23-7.25 (dd, 1H) J = 2, 1.3 Hz), 7.27 (d, 1H, J = 2.4 Hz), 7.34 (d, 1H, J = 15.6 Hz), 7.47-7.50 (m, 1H), 7.80 (d, 1H, J = 15.6 Hz), 8.29-8.32 (dt, 1H, J = 6, 2 Hz), 8.81 (d, 1H, J = 3.6 Hz), 9.24 (brs, 1H); ¹³C-NMR (CDCl₃, 400 MHz) δ 56.00, 110.08, 115.09, 118.88, 123.92, 126.90, 136.02, 146.50, 147.04, 149.00, 149.42, 152.67, 189.01; HMRS (esi) m/z calcd for [M+H] 256.0974, found 256.0961.

4.1.1.2 (*E*)-3-(3-ethoxy-4-hydroxyphenyl)-1-(pyridin-3-yl)prop-2-en-1-one (**2**)

Compound **2** was obtained from compound **12**; eluting mixture mobile phase dichloromethane / toluene / methanol (9:0.8:0.2); yellow solid; 55% yield; mp = 179-181 °C; ¹H-NMR (CDCl₃, 400 MHz) δ 1.37 (t, 3H, J = 6.8 Hz), 4.11-4.16 (q, 2H, J = 6.8, 6.8 Hz), 6.86 (d, 1H, J = 8 Hz), 7.29 (d, 1H, J = 7.6 Hz), 7.54 (s, 1H), 7.58-7.61 (dd, 1H, J = 5.2, 2.4 Hz), 7.69-7.80 (q, 2H, J = 15.2, 12.4 Hz), 8.43 (d, 1H, J = 7.6 Hz), 8.81 (d, 1H, J = 8.8 Hz), 9.33 (s, 1H), 9.68 (s, 1H); ¹³C-NMR (DMSO-*d*₆, 100 MHz) δ 14.67, 64.01, 112.90, 115.64, 118.29, 123.86, 124.63, 126.05, 133.16, 135.78, 145.76, 147.17, 149.56, 150.30, 153.02, 188.07; HMRS (esi) m/z calcd for [M+H] 270.1130, found 270.1147.

4.1.1.3 (*E*)-3-(3,4-dihydroxyphenyl)-1-(pyridin-3-yl)prop-2-en-1-one (**3**)

Compound **3** was obtained from compound **13**; eluting mixture mobile phase dichloromethane / methanol (9.5:0.5); yellow solid; 58% yield; mp = 237-239 °C; ¹H-NMR (DMSO-*d*₆, 400 MHz) δ 6.81 (d, 1H, J = 8 Hz), 7.20-7.23 (dd, 1H, J = 8, 2 Hz), 7.28 (d, 1H, J = 2), 7.56-7.59 (m, 1H) dd, J = 12.8, 3.2 Hz), 7.64 (s, 2H), 8.40-8.43 (dt, 1H, J = 8, 2), 8.79-8.80 (dd, 1H, J = 4.8, 1.6 Hz), 9.26 (d, 1H, J = 1.6 Hz); ¹³C-NMR (DMSO-*d*₆, 100 MHz) δ 115.75, 115.82, 118.20, 122.57, 123.87, 126.08, 133.23, 135.78, 145.64, 145.79, 149.12, 149.47, 153.00, 188.15; HMRS (esi) m/z calcd for [M+H] 242.0817, found 242.0802.

4.1.1.4 (*E*)-3-(4-hydroxyphenyl)-1-(pyridin-3-yl)prop-2-en-1-one (**4**)

Compound **4** was obtained from compound **14**; eluting mixture mobile phase dichloromethane / methanol (9.5:0.5); yellow solid; 72% yield; mp = 213-215 °C; ¹H-NMR (CD₃OD-*d*₄, 400 MHz) δ 6.84 (d, 1H, J = 8.4 Hz), 7.56-7.66 (m, 4H), 7.80 (d, 1H, J = 15.6 Hz), 8.45 (d, 1H, J = 8 Hz), 8.83

(d, 1H, J = 3.6 Hz), 8.18 (s, 1H); ¹³C-NMR (DMSO-*d*₆, 100 MHz) δ 115.84, 118.23, 123.86, 125.58, 131.30, 133.14, 135.77, 145.29, 149.49, 153.02, 160.42, 188.14; HMRS (esi) m/z calcd for [M+H] 226.0868, found 226.0857.

4.1.1.5. (*E*)-3-(3-hydroxyphenyl)-1-(pyridin-3-yl)prop-2-en-1-one (**5**):

Compound **5** was obtained from compound **15**; eluting mixture mobile phase dichloromethane / methanol (9.5:0.5); yellow solid; 41% yield; mp = 209-211 °C; ¹H-NMR (CD₃OD-*d*₄, 400 MHz) δ 6.69 (m, 1H), 6.78-6.89 (dt, 1H, J = 7.2, 2.4 Hz), 7.06-7.07 (m, 1H), 7.15-7.20 (m, 2H), 7.53-7.55 (dd, 1H, J = 5.0, 3.2 Hz), 7.58 (d, J = 5.6 Hz), 7.68 (d, 1H, J = 15.6 Hz), 8.37-8.40 (dt, 1H, J = 8.5, 2 Hz), 8.68 (s, 1H), 9.11 (s, 1H); ¹³C-NMR (DMSO-*d*₆, 100 MHz) δ 116.11, 119.01, 123.55, 125.77, 131.01, 134.00, 135.86, 144.92, 149.86, 152.74, 160.90, 188.44; HMRS (esi) m/z calcd for [M+H] 226.0868, found 226.0884.

4.1.2 General procedure for the synthesis of compounds **6-10**

To a solution of the appropriate aldehyde (1 eq) in dichloromethane at room temperature (if the aldehyde is not completely soluble it is possible to add some drops of DMF), pyridinium paratoluenesulfonate was added as a catalyst, followed by a drop-wise addition of a solution of dihydropyran (1 eq) in DCM. The mixture was stirred at room temperature until the starting materials disappeared. The organic mixture was washed three times with water, dried over magnesium sulphate and concentrated to give an orange to brown oil, which was used in the next steps without further purification.

4.1.2.1 3-methoxy-4-((tetrahydro-2H-pyran-2-yl)oxy)benzaldehyde (**6**)

Compound **6** was obtained from 4-Hydroxy-3-methoxybenzaldehyde; yellow oil; HMRS (esi) m/z calcd for [M+H] 237.1127, found 237.1143.

4.1.2.2 3-ethoxy-4-((tetrahydro-2H-pyran-2-yl)oxy)benzaldehyde (**7**)

Compound **7** was obtained from 4-Hydroxy-3-methoxybenzaldehyde; yellow oil; HMRS (esi) m/z calcd for [M+H] 251.1283, found 251.1297.

4.1.2.3 3,4-bis((tetrahydro-2H-pyran-2-yl)oxy)benzaldehyde (**8**)

Compound **8** was obtained from 3,4-dihydroxybenzaldehyde; HMRS (esi) m/z calcd for [M+H] 307.1545, found 307.1531.

4.1.2.4 4-((tetrahydro-2H-pyran-2-yl)oxy)benzaldehyde (**9**)

Compound **9** was obtained from 3-dihydroxybenzaldehyde; yellow oil; HMRS (esi) m/z calcd for [M+H] 207.1021, found 207.1045.

4.1.2.5 3-((tetrahydro-2H-pyran-2-yl)oxy)benzaldehyde (**10**)

Compound **10** was obtained from 4-dihydroxybenzaldehyde; yellow oil; HMRS (esi) m/z calcd for $[M+H]$ 207.1021, found 207.1033.

4.1.3 General procedure for the synthesis of compounds **11-15**

To a solution of the appropriate aldehydes **6-10** (1 eq) in NaOH aq 2.5 M, 3-acetylpyridine (1 eq) was added dropwise and the color of the solution turned ~~from~~ from yellow to intense red; the resulting mixture was stirred overnight at room temperature. The solvent was removed *in vacuo* and the obtained residue was purified through flash chromatography.

4.1.3.1 (*E*)-3-(3-methoxy-4-((tetrahydro-2H-pyran-2-yl)oxy)phenyl)-1-(pyridin-3-yl)prop-2-en-1-one (**11**)

Compound **11** was obtained from compound **6**; eluting mixture dichloromethane / methanol (9:1); yellow oil; 51% yield; $^1\text{H-NMR}$ (CdCl_3 , 400 MHz) δ 1.61-1.68 (m, 2H), 1.77-1.88 (m, 2H), 1.91-2.01 (m, 2H), 3.52-3.59 (m, 1H), 3.81-3.87 (m, 1H), 3.91 (s, 3H), 5.29-5.38 (m, 1H), 6.84 (d, 1H), 7.28-7.51 (d, 4H), 7.82-7.95 (d, 1H), 8.49 (d, 1H), 8.86 (m, 1H), 9.35 (d, 1H); HMRS (esi) m/z calcd for $[M+H]$ 340.1549, found 340.1557.

4.1.3.2 (*E*)-3-(3-ethoxy-4-((tetrahydro-2H-pyran-2-yl)oxy)phenyl)-1-(pyridin-3-yl)prop-2-en-1-one (**12**)

Compound **12** was obtained from compound **7**; eluting mixture dichloromethane / methanol (9:1); yellow oil; 60% yield; $^1\text{H-NMR}$ (CdCl_3 , 400 MHz) δ 1.42-1.56 (m, 4H), 1.61-1.71 (m, 2H), 1.72-1.79 (m, 1H), 2.05-2.12 (m, 1H), 3.33-3.41 (m, 1H), 3.78-3.85 (m, 1H), 3.91 (s, 3H), 5.22-5.27 (m, 1H), 6.84 (d, 1H), 7.28-7.51 (d, 4H), 7.82-7.95 (d, 1H), 8.49 (d, 1H), 8.86 (m, 1H), 9.35 (d, 1H); HMRS (esi) m/z calcd for $[M+H]$ 354.1705, found 354.1698.

4.1.3.3 (*E*)-3-(3,4-bis((tetrahydro-2H-pyran-2-yl)oxy)phenyl)-1-(pyridin-3-yl)prop-2-en-1-one (**13**)

Compound **13** was obtained from compound **8**; eluting mixture dichloromethane/methanol (9/1); yellow oil; 45% yield; $^1\text{H-NMR}$ (CdCl_3 , 400 MHz) δ 1.54-1.89 (m, 8H), 2.06-2.47 (m, 4H), 3.77-3.95 (m, 2H), 5.30-5.51 (m, 2H), 5.81-5.92 (m, 2H), 6.89 (d, 1H), 7.31-7.55 (d, 4H), 7.83-7.95 (d, 1H), 8.44 (d, 1H), 8.91 (m, 1H), 9.32 (d, 1H); HMRS (esi) m/z calcd for $[M+H]$ 410.1967, found 410.1951.

4.1.3.4 (*E*)-1-(pyridin-3-yl)-3-(4-((tetrahydro-2H-pyran-2-yl)oxy)phenyl)prop-2-en-1-one (**14**)

Compound **14** was obtained from compound **9**; eluting mixture dichloromethane / toluene / methanol (8:1:1); yellow oil; 38 % yield; $^1\text{H-NMR}$ (CdCl_3 , 400 MHz) δ 1.49-1.57 (m, 2H), 1.64-1.69 (m, 2H), 1.77-1.99 (m, 2H), 3.79-3.84 (m, 1H), 3.91-3.95 (m, 1H), 5.89-5.94 (m, 1H), 6.92 (d, 1H), 7.34-7.58 (d, 4H), 7.84-91 (d, 2H), 8.32 (d, 1H), 8.82 (m, 1H), 9.23 (d, 1H); HMRS (esi) m/z calcd for $[M+H]$ 310.1443, found 310.1432.

4.1.3.5 (E)-1-(pyridin-3-yl)-3-(3-((tetrahydro-2H-pyran-2-yl)oxy)phenyl)prop-2-en-1-one (15)

Compound **15** was obtained from compound **10**; eluting mixture dichloromethane / methanol (9:1); yellow oil; 42 % yield; $^1\text{H-NMR}$ (CdCl_3 , 400 MHz) δ 1.53-1.62 (m, 2H), 1.61-1.73 (m, 2H), 1.81-1.95 (m, 2H), 3.61-3.64 (m, 1H), 3.89-3.94 (m, 1H), 5.67-5.71 (m, 1H), 6.72 (d, 1H), 6.98 (d, 1H), 7.13- 7.33 (m, 4H), 7.60 (d, 1H), 7.82 (m, 1H), 8.35 (d, 1H), 8.81 (d, 1H); HMRS (esi) m/z calcd for $[\text{M}+\text{H}]$ 310.1443, found 310.1458.

4.1.4 Autoxidation experiments

Autoxidation experiments were performed in a two-channel oxygen-uptake apparatus based on a Validyne DP 15 differential pressure transducer built in our laboratory and described previously.[70-72] The antioxidant activity of the title compounds was evaluated by studying the inhibition of the thermally initiated autoxidation of cumene (3.6 M) or styrene (4.3 M) in chlorobenzene or THF (3.1 M) in aqueous phosphate buffer (pH 7.4). In a typical experiment, an air-saturated mixture of the oxidizable substrate and the solvent, cumene or styrene/chlorobenzene 1:1 (v/v) containing AIBN (0.05 M) as initiator or THF/water 1:3 (v/v) containing the buffer (0.1M) and AAPH (25mM) as initiator was equilibrated with an identical reference solution containing an excess of 2,2,5,7,8-pentamethyl-6-chromanol. After equilibration, and when a constant O_2 consumption was reached, 10-50 μL of a concentrated solution of the antioxidant was injected into the sample flask and oxygen consumption in the sample was measured. From the slope of oxygen consumption in the absence of antioxidant ($-\text{d}[\text{O}_2]/\text{dt})_0 = R_{\text{ox}0}$) and during the inhibited period ($-\text{d}[\text{O}_2]/\text{dt} = R_{\text{ox}}$), k_{inh} values were obtained by fitting to Eq. (1), while the n coefficients were determined from the length of the inhibited period (τ) by using Eq. (2), from the known rate of radical production by AIBN or AAPH (initiation rate, R_i).[73]

$$\frac{R_{\text{ox}0}}{R_{\text{ox}}} - \frac{R_{\text{ox}}}{R_{\text{ox}0}} = \frac{nk_{\text{inh}}[\text{AH}]_0}{\sqrt{2K_i R_i}} \quad \text{Eq. (1)}$$

$$n = \frac{R_i \tau}{[\text{antioxidant}]} \quad \text{Eq. (2)}$$

The $2k_t$ values of cumene, styrene and THF at 303K are $4.2 \times 10^7 \times 10^7$, $4.6 \times 10^4 \times 10^4$ and $6.6 \times 10^7 \times 10^7 \text{ M}^{-1}\text{s}^{-1}$, respectively. The value of R_i was determined under each experimental condition by using PMHC (2,2,5,7,8-pentamethyl-6-chromanol) or Trolox ((\pm)-6-Hydroxy-2,5,7,8-tetramethylchromane-2-carboxylic acid) as a reference antioxidant: system = chlorobenzene / cumene, $R_i 4.3 \times 10^{-9} \text{ M s}^{-1}$; system = buffer pH 7.4/THF, $R_i 7.3 \times 10^{-9} \text{ M s}^{-1}$.

4.1.5 UV-vis Spectroscopy

UV-vis absorption spectra were recorded at room temperature by using a Jasco V550 double-beam spectrometer with baseline correction. The solutions were placed in quartz absorption cuvettes with a pathlength of 10 mm and a chamber volume of 3.5 mL. Stock solutions of compound **3** (1 mM) and CuCl₂ (1 mM) in methanol were freshly prepared and purged with nitrogen to prevent oxidation. Under typical settings a fixed concentration of compound **3** (5 to 15 × 10⁻⁶ M) was added of growing amounts of CuCl₂ (up to 3 equivalents), oxygen was removed by purging with N₂ and the spectra (200-600 nm) were recorded vs neat methanol (solvent). At each concentration setting the spectra of compound **3** and of CuCl₂ at the same concentration in methanol were numerically subtracted from that of the mixture to obtain the differential spectra. Molar extinction coefficients for **3** in methanol were determined from calibration plots at 6 different concentrations (2-30 × 10⁻⁶ M) using Lambert-Beer's law.

4.2 Biology

4.2.1 Luminescence Assay for GSK-3β inhibition determination

Assays were performed in 50 mM HEPES, 1 mM EDTA, 1 mM EGTA, and 15 mM magnesium acetate pH 7.5 assay buffer, using white 96-well plates. In a typical assay, 10 μL of test compound (dissolved in DMSO at 1 mM concentration and diluted in assay buffer to the desired concentration) and 10 μL (20 ng) of enzyme were added to each well, followed by 20 μL of assay buffer containing 25 μM GSM substrate and 1 μM ATP. The final DMSO concentration in the reaction mixture did not exceed 1%. After a 30-min incubation at 30 °C, the enzymatic reaction was stopped with 40 μL of Kinase-Glo reagent. After 10 min, luminescence in the entire visible range was recorded using a Victor™ X3 Perkin Elmer multimode reader. The activity is proportional to the difference between the total and consumed ATP. The inhibitory activities were calculated on the basis of maximal kinase and luciferase activities measured in the absence of inhibitor and in the presence of reference compound inhibitor SB-415826,[74] at total inhibition concentration, respectively. The linear regression parameters were determined and the IC₅₀ extrapolated (GraphPad Prism 4.0, GraphPad Software Inc.).

Since the assay is based on the direct quantification of ATP cofactor by luciferase enzyme, for compound **3** the activity was also evaluated in absence of GSK-3β and no interaction was detected between compound **3** and luciferase up to 3 mM compound concentration.

4.2.2 Determination of the inhibitory activity on A β ₄₂ self-aggregation

As reported in a previously published protocol,[41] a 1,1,1,3,3,3,-hexafluoro-2-propanol (HFIP) pretreated A β ₄₂ sample (Bachem AG, Switzerland) was solubilized in a CH₃CN/0.3 mM Na₂CO₃/250 mM NaOH (48.4:48.4:3.2) mixture to obtain a 500 μ M solution. Experiments were performed by diluting the peptide to a final concentration of 50 μ M with 10 mM phosphate buffer (pH = 8.0) containing 10 mM NaCl, and incubating the diluted solution at 30°C. In these conditions a reproducible aggregation kinetic was obtained.[41] For inhibition studies, A β ₄₂ (50 μ M) was incubated in 10 mM phosphate buffer (pH = 8.0) containing 10 mM NaCl, at 30°C (pH = 8.0) in the absence and in the presence of compounds **1-5** (50 μ M, A β /inhibitor = 1/1). Blanks containing the inhibitors were also prepared and tested. Amyloid fibril formation was quantified by a ThT-method.[69, 75]

Fluorescence intensities in the absence and in the presence of inhibitor were compared and the percent inhibition due to the presence of the inhibitor was calculated. For the determination of the IC₅₀ value, increasing concentrations of **5**, able to inhibit amyloid aggregation by 20-80%, were evaluated.

To exclude any spectral interference between ThT and compound **5**, fluorescence intensities recorded before and after the addition of **5** to a pre-aggregated A β ₄₂ sample were compared.

4.2.3 Determination of the inhibitory activity on Tg2

Kinetic runs were recorded in triplicate on a BioTek Synergy H4 hybrid reader microplate reader in absorbance mode at 405 nm and 25°C, in a buffer composed of 111 mM MOPS (pH 7.0), 3.33 mM CaCl₂, and 0.05 mM EDTA. All aqueous solutions were prepared using deionised water. Each kinetic assay was performed using 900 μ L buffer, 25 μ L of a DMSO stock solution of substrate *N*-Cbz-Glu(γ -*p*-nitrophenylester)Gly [76] (1 mg mL⁻¹, 2.2 mM), 50 μ L of a solution of recombinant human TG2 (hTG2) at 0.05 U mL⁻¹ (final concentration of 2.5 mU mL⁻¹) and 0-25 μ L of a DMSO stock solution of inhibitor (contingent on solubility; the highest concentration tested ranged between 186 and 222 μ M). The volume of DMSO was then adjusted so that it represented 5% of the final volume. The reaction was initiated with the addition of hTG2 (expressed and purified according to a literature protocol [77]), and the increase in absorbance was monitored over 10 minutes; initial[77]), and the increase in absorbance was monitored over 10 minutes. Initial rates were measured over the first minute of absorbance change, corresponding to the linear portion of the curve. IC₅₀ values were obtained as the negative x-intercept of a Dixon plot (reciprocal of initial rates vs. inhibitor

concentration), from the average of two triplicate runs. The reported error was the standard error of the mean.

4.2.4 Cell viability

For neuronal cytotoxicity studies, immature primary cortical neurons (E17) were isolated as described[65] and plated at a density of 10^6 cells/ml in 96-well plates. The next day cells were rinsed and then placed in medium containing 5 mM glutamate. Increasing concentrations of compound **3** were added at the time of glutamate treatment. The next day, cell viability was assessed by the MTT assay (Sigma).

4.2.5 PAMPA assay

To predict passive blood-brain penetration modification of the PAMPA has been used based on reported protocol.[66, 67] The filter membrane of the donor plate was coated with PBL (Polar Brain Lipid, Avanti, USA) in dodecane (4 μ l of 20 mg/ml PBL in dodecane) and the acceptor well was filled with 300 μ l of PBS pH 7.4 buffer (V_D). Tested compounds were dissolved first in DMSO and that diluted with PBS pH 7.4 to reach the final concentration 100 μ M in the donor well. Concentration of DMSO did not exceed 0.5% (V/V) in the donor solution. 300 μ L of the donor solution was added to the donor wells (V_A) and the donor filter plate was carefully put on the acceptor plate so that coated membrane was “in touch” with both donor solution and acceptor buffer. Test compound diffused from the donor well through the lipid membrane (Area = 0.28 cm²) to the acceptor well. The concentration of the drug in both donor and the acceptor wells was assessed after 3, 4, 5 and 6 h of incubation in quadruplicate using the UV plate reader Synergy HT (Biotek, USA) at the maximum absorption wavelength of each compound. Concentration of the compounds was calculated from the standard curve and expressed as permeability (Pe) value according to Eq. 3:[78, 79]

$$\log \frac{C_A}{C_D} = \log \left\{ \frac{C_D}{C_D} \times \left(1 - \frac{[C_D]_{\text{initial}}}{[C_D]_{\text{initial}}} \right) \right\} \times h = \left(\frac{C_A}{C_D} \times \frac{1}{1 - \frac{[C_D]_{\text{initial}}}{[C_D]_{\text{initial}}}} \right) \quad (\text{Eq. 3})$$

Acknowledgements

This work was supported by the University of Bologna (RFO and FIRB FFBO123154 project NANOX), the Italian Ministry for Education, Universities and Research (MIUR), The Alzheimer Trento Onlus with the legato Baldrachi (to M.B and A.M.), the Natural Sciences and Engineering

Research Council of Canada (to KYPA and JWK) and MH CZ - DRO (UHHK 00179906) for the financial support. AM thanks Dr. Martina Battistini for excellent technical support.

Abbreviations

AChE, Acetylcholinesterase; AChEI, Acetylcholinesterase inhibitor; AD, Alzheimer's disease; AIBN, Azobisisobutyronitrile; APP, amyloid precursor protein; A β , amyloid beta; BACE-1, β -secretase 1; BBB, blood-brain barrier; BDE, bond dissociation enthalpy; CNS, central nervous system; DIV1, day *in vitro*; ED, electron donating; EPT, electron-proton transfer; ET, electron transfer; EW, electron withdrawing; FDA, food and drug administration; GSK-3 β , glycogen synthase kinase 3 β ; MTT, 3-(4,5-dimethylthiazol-2-yl)-2,5-diphenyltetrazolium bromide; NFT, neurofibrillary tangles; NMDA, N-methyl D-aspartate; PAMPA, parallel artificial membrane permeation assay; PhCl, chlorobenzene; PT, proton transfer; ROS, reactive oxygen species; MTL, multitarget ligand; SAR, structure-activity relationships; Tg2, transglutaminase 2; ThT, thioflavin T

Bibliography

- [1] R. Morphy, Z. Rankovic, Designed multiple ligands. An emerging drug discovery paradigm, *J Med Chem*, 48 (2005) 6523-6543.
- [2] M.L. Bolognesi, Polypharmacology in a single drug: multitarget drugs, *Curr Med Chem*, 20 (2013) 1639-1645.
- [3] A. Cavalli, M.L. Bolognesi, A. Minarini, M. Rosini, V. Tumiatti, M. Recanatini, C. Melchiorre, Multi-target-directed ligands to combat neurodegenerative diseases, *J Med Chem*, 51 (2008) 347-372.
- [4] E. Karran, M. Mercken, B. De Strooper, The amyloid cascade hypothesis for Alzheimer's disease: an appraisal for the development of therapeutics, *Nat Rev Drug Discov*, 10 (2011) 698-712.
- [5] R.B. Maccioni, G. Farías, I. Morales, L. Navarrete, The revitalized tau hypothesis on Alzheimer's disease, *Arch Med Res*, 41 (2010) 226-231.
- [6] J.J. Palop, J. Chin, L. Mucke, A network dysfunction perspective on neurodegenerative diseases, *Nature*, 443 (2006) 768-773.
- [7] A. Wimo, and Prince, M., World Alzheimer Report 2010: The Global Economic Impact of Dementia, London: Alzheimer's Disease International, 2010, pp. 1-56.
- [8] J.L. Cummings, T. Morstorf, K. Zhong, Alzheimer's disease drug-development pipeline: few candidates, frequent failures, *Alzheimers Res Ther*, 6 (2014) 37.
- [9] S.O. Bachurin, E.V. Bovina, A.A. Ustyugov, Drugs in Clinical Trials for Alzheimer's Disease: The Major Trends, *Med Res Rev*, (2017).
- [10] L. Ismaili, B. Refouvelet, M. Benchekroun, S. Brogi, M. Brindisi, S. Gemma, G. Campiani, S. Filipic, D. Agbaba, G. Esteban, M. Unzeta, K. Nikolic, S. Butini, J. Marco-Contelles, Multitarget compounds bearing tacrine- and donepezil-like structural and functional motifs for the potential treatment of Alzheimer's disease, *Prog Neurobiol*, (2016).
- [11] V. Tumiatti, A. Minarini, M.L. Bolognesi, A. Milelli, M. Rosini, C. Melchiorre, Tacrine derivatives and Alzheimer's disease, *Curr Med Chem*, 17 (2010) 1825-1838.
- [12] A. Minarini, A. Milelli, E. Simoni, M. Rosini, M.L. Bolognesi, C. Marchetti, V. Tumiatti, Multifunctional tacrine derivatives in Alzheimer's disease, *Curr Top Med Chem*, 13 (2013) 1771-1786.
- [13] F. Prati, A. De Simone, P. Bisignano, A. Armirotti, M. Summa, D. Pizzirani, R. Scarpelli, D.I. Perez, V. Andrisano, A. Perez-Castillo, B. Monti, F. Massenzio, L. Polito, M. Racchi, A.D. Favia, G. Bottegoni, A. Martinez, M.L. Bolognesi, A. Cavalli, Multitarget drug discovery for Alzheimer's disease: triazinones as BACE-1 and GSK-3 β inhibitors, *Angew Chem Int Ed Engl*, 54 (2015) 1578-1582.

- [14] F. Prati, A. De Simone, A. Armirotti, M. Summa, D. Pizzirani, R. Scarpelli, S.M. Bertozzi, D.I. Perez, V. Andrisano, A. Perez-Castillo, B. Monti, F. Massenzio, L. Polito, M. Racchi, P. Sabatino, G. Bottegoni, A. Martinez, A. Cavalli, M.L. Bolognesi, 3,4-Dihydro-1,3,5-triazin-2(1H)-ones as the First Dual BACE-1/GSK-3 β Fragment Hits against Alzheimer's Disease, *ACS Chem Neurosci*, 6 (2015) 1665-1682.
- [15] R. Yan, R. Vassar, Targeting the β secretase BACE1 for Alzheimer's disease therapy, *Lancet Neurol*, 13 (2014) 319-329.
- [16] C. Hooper, R. Killick, S. Lovestone, The GSK3 hypothesis of Alzheimer's disease, *J Neurochem*, 104 (2008) 1433-1439.
- [17] M. Llorens-Martín, J. Jurado, F. Hernández, J. Avila, GSK-3 β , a pivotal kinase in Alzheimer disease, *Front Mol Neurosci*, 7 (2014) 46.
- [18] M.E. Kennedy, A.W. Stamford, X. Chen, K. Cox, J.N. Cumming, M.F. Dockendorf, M. Egan, L. Ereshefsky, R.A. Hodgson, L.A. Hyde, S. Jhee, H.J. Kleijn, R. Kuvelkar, W. Li, B.A. Mattson, H. Mei, J. Palcza, J.D. Scott, M. Tanen, M.D. Troyer, J.L. Tseng, J.A. Stone, E.M. Parker, M.S. Forman, The BACE1 inhibitor verubecestat (MK-8931) reduces CNS β -amyloid in animal models and in Alzheimer's disease patients, *Sci Transl Med*, 8 (2016) 363ra150.
- [19] H. Ma, S. Lesné, L. Kotilinek, J.V. Steidl-Nichols, M. Sherman, L. Younkin, S. Younkin, C. Forster, N. Sergeant, A. Delacourte, R. Vassar, M. Citron, P. Kofuji, L.M. Boland, K.H. Ashe, Involvement of beta-site APP cleaving enzyme 1 (BACE1) in amyloid precursor protein-mediated enhancement of memory and activity-dependent synaptic plasticity, *Proc Natl Acad Sci U S A*, 104 (2007) 8167-8172.
- [20] S. Barão, D. Moechars, S.F. Lichtenthaler, B. De Strooper, BACE1 Physiological Functions May Limit Its Use as Therapeutic Target for Alzheimer's Disease, *Trends Neurosci*, 39 (2016) 158-169.
- [21] T. Mohamed, A. Shakeri, P.P. Rao, Amyloid cascade in Alzheimer's disease: Recent advances in medicinal chemistry, *Eur J Med Chem*, 113 (2016) 258-272.
- [22] J. Sevigny, P. Chiao, T. Bussière, P.H. Weinreb, L. Williams, M. Maier, R. Dunstan, S. Salloway, T. Chen, Y. Ling, J. O'Gorman, F. Qian, M. Arastu, M. Li, S. Chollate, M.S. Brennan, O. Quintero-Monzon, R.H. Scannevin, H.M. Arnold, T. Engber, K. Rhodes, J. Ferrero, Y. Hang, A. Mikulskis, J. Grimm, C. Hock, R.M. Nitsch, A. Sandrock, The antibody aducanumab reduces A β plaques in Alzheimer's disease, *Nature*, 537 (2016) 50-56.
- [23] D.J. Selkoe, J. Hardy, The amyloid hypothesis of Alzheimer's disease at 25 years, *EMBO Mol Med*, 8 (2016) 595-608.
- [24] M. Rosini, E. Simoni, A. Milelli, A. Minarini, C. Melchiorre, Oxidative stress in Alzheimer's disease: are we connecting the dots?, *J Med Chem*, 57 (2014) 2821-2831.
- [25] G. Perry, A.D. Cash, M.A. Smith, Alzheimer Disease and Oxidative Stress, *J Biomed Biotechnol*, 2 (2002) 120-123.
- [26] Y. Zhao, B. Zhao, Oxidative stress and the pathogenesis of Alzheimer's disease, *Oxid Med Cell Longev*, 2013 (2013) 316523.
- [27] S.M. Alavi Naini, N. Soussi-Yanicostas, Tau Hyperphosphorylation and Oxidative Stress, a Critical Vicious Circle in Neurodegenerative Tauopathies?, *Oxid Med Cell Longev*, 2015 (2015) 151979.
- [28] B. Su, X. Wang, H.G. Lee, M. Tabaton, G. Perry, M.A. Smith, X. Zhu, Chronic oxidative stress causes increased tau phosphorylation in M17 neuroblastoma cells, *Neurosci Lett*, 468 (2010) 267-271.
- [29] M.A. Lovell, S. Xiong, C. Xie, P. Davies, W.R. Markesbery, Induction of hyperphosphorylated tau in primary rat cortical neuron cultures mediated by oxidative stress and glycogen synthase kinase-3, *J Alzheimers Dis*, 6 (2004) 659-671; discussion 673-681.
- [30] C.X. Peng, J. Hu, D. Liu, X.P. Hong, Y.Y. Wu, L.Q. Zhu, J.Z. Wang, Disease-modified glycogen synthase kinase-3 β intervention by melatonin arrests the pathology and memory deficits in an Alzheimer's animal model, *Neurobiol Aging*, 34 (2013) 1555-1563.
- [31] G. Scapagnini, D.A. Butterfield, C. Colombrita, R. Sultana, A. Pascale, V. Calabrese, Ethyl ferulate, a lipophilic polyphenol, induces HO-1 and protects rat neurons against oxidative stress, *Antioxid Redox Signal*, 6 (2004) 811-818.
- [32] B.A. Cussac M, *Chimica Therapeutica*, 1967, pp. 101.
- [33] *JpnKokai Tokyo Koho* (1992), JP 04154720 A 19920527.

- [34] C. Zhuang, W. Zhang, C. Sheng, C. Xing, Z. Miao, Chalcone: A Privileged Structure in Medicinal Chemistry, *Chem Rev*, (2017).
- [35] R.M. Di Martino, A. De Simone, V. Andrisano, P. Bisignano, A. Bisi, S. Gobbi, A. Rampa, R. Fato, C. Bergamini, D.I. Perez, A. Martinez, G. Bottegoni, A. Cavalli, F. Belluti, Versatility of the Curcumin Scaffold: Discovery of Potent and Balanced Dual BACE-1 and GSK-3 β Inhibitors, *J Med Chem*, 59 (2016) 531-544.
- [36] A.A. Reinke, J.E. Gestwicki, Structure-activity relationships of amyloid beta-aggregation inhibitors based on curcumin: influence of linker length and flexibility, *Chem Biol Drug Des*, 70 (2007) 206-215.
- [37] C. Pardin, J.N. Pelletier, W.D. Lubell, J.W. Keillor, Cinnamoyl inhibitors of tissue transglutaminase, *J Org Chem*, 73 (2008) 5766-5775.
- [38] M. Lesort, J. Tucholski, M.L. Miller, G.V. Johnson, Tissue transglutaminase: a possible role in neurodegenerative diseases, *Prog Neurobiol*, 61 (2000) 439-463.
- [39] A. Baki, A. Bielik, L. Molnár, G. Szendrei, G.M. Keserü, A high throughput luminescent assay for glycogen synthase kinase-3 β inhibitors, *Assay Drug Dev Technol*, 5 (2007) 75-83.
- [40] L. Avrahami, A. Licht-Murava, M. Eisenstein, H. Eldar-Finkelman, GSK-3 inhibition: achieving moderate efficacy with high selectivity, *Biochim Biophys Acta*, 1834 (2013) 1410-1414.
- [41] M. Bartolini, C. Bertucci, M.L. Bolognesi, A. Cavalli, C. Melchiorre, V. Andrisano, Insight into the kinetic of amyloid beta (1-42) peptide self-aggregation: elucidation of inhibitors' mechanism of action, *Chembiochem*, 8 (2007) 2152-2161.
- [42] Q.I. Churches, J. Caine, K. Cavanagh, V.C. Epa, L. Waddington, C.E. Tranberg, A.G. Meyer, J.N. Varghese, V. Streltsov, P.J. Duggan, Naturally occurring polyphenolic inhibitors of amyloid beta aggregation, *Bioorg Med Chem Lett*, 24 (2014) 3108-3112.
- [43] X. Chao, X. He, Y. Yang, X. Zhou, M. Jin, S. Liu, Z. Cheng, P. Liu, Y. Wang, J. Yu, Y. Tan, Y. Huang, J. Qin, S. Rapposelli, R. Pi, Design, synthesis and pharmacological evaluation of novel tacrine-caffeic acid hybrids as multi-targeted compounds against Alzheimer's disease, *Bioorg Med Chem Lett*, 22 (2012) 6498-6502.
- [44] A. Minarini, A. Milelli, V. Tumiatti, M. Rosini, E. Simoni, M.L. Bolognesi, V. Andrisano, M. Bartolini, E. Motori, C. Angeloni, S. Hrelia, Cystamine-tacrine dimer: a new multi-target-directed ligand as potential therapeutic agent for Alzheimer's disease treatment, *Neuropharmacology*, 62 (2012) 997-1003.
- [45] E. Simoni, M.M. Serafini, M. Bartolini, R. Caporaso, A. Pinto, D. Necchi, J. Fiori, V. Andrisano, A. Minarini, C. Lanni, M. Rosini, Nature-Inspired Multifunctional Ligands: Focusing on Amyloid-Based Molecular Mechanisms of Alzheimer's Disease, *ChemMedChem*, 11 (2016) 1309-1317.
- [46] S. Ayton, P. Lei, A.I. Bush, Biomaterials and their therapeutic implications in Alzheimer's disease, *Neurotherapeutics*, 12 (2015) 109-120.
- [47] J.S. Cristóvão, R. Santos, C.M. Gomes, Metals and Neuronal Metal Binding Proteins Implicated in Alzheimer's Disease, *Oxid Med Cell Longev*, 2016 (2016) 9812178.
- [48] X. Huang, M.P. Cuajungco, C.S. Atwood, M.A. Hartshorn, J.D. Tyndall, G.R. Hanson, K.C. Stokes, M. Leopold, G. Multhaup, L.E. Goldstein, R.C. Scarpa, A.J. Saunders, J. Lim, R.D. Moir, C. Glabe, E.F. Bowden, C.L. Masters, D.P. Fairlie, R.E. Tanzi, A.I. Bush, Cu(II) potentiation of alzheimer abeta neurotoxicity. Correlation with cell-free hydrogen peroxide production and metal reduction, *J Biol Chem*, 274 (1999) 37111-37116.
- [49] C.J. Sarell, S.R. Wilkinson, J.H. Viles, Substoichiometric levels of Cu²⁺ ions accelerate the kinetics of fiber formation and promote cell toxicity of amyloid- β from Alzheimer disease, *J Biol Chem*, 285 (2010) 41533-41540.
- [50] v.d.B.M.G. Constant, Determination of the complexing capacity and conditional stability constants of complexes of copper(II) with natural organic ligands in seawater by cathodic stripping voltammetry of copper-catechol complex ions, *Marine Chemistry*, 1984, pp. 1-18.
- [51] R. Amorati, L. Valgimigli, Advantages and limitations of common testing methods for antioxidants, *Free Radic Res*, 49 (2015) 633-649.
- [52] R. Matera, S. Gabbanini, S. Berretti, R. Amorati, G.R. De Nicola, R. Iori, L. Valgimigli, Acylated anthocyanins from sprouts of *Raphanus sativus* cv. Sango: isolation, structure elucidation and antioxidant activity, *Food Chem*, 166 (2015) 397-406.
- [53] R. Amorati, L. Valgimigli, Modulation of the antioxidant activity of phenols by non-covalent interactions, *Org Biomol Chem*, 10 (2012) 4147-4158.

- [54] R. Amorati, S. Menichetti, E. Mileo, G.F. Pedulli, C. Viglianisi, Hydrogen-atom transfer reactions from ortho-alkoxy-substituted phenols: an experimental approach, *Chemistry*, 15 (2009) 4402-4410.
- [55] L. Valgimigli, D.A. Pratt, Maximizing the reactivity of phenolic and aminic radical-trapping antioxidants: just add nitrogen!, *Acc Chem Res*, 48 (2015) 966-975.
- [56] R. Amorati, G.F. Pedulli, L. Cabrini, L. Zambonin, L. Landi, Solvent and pH effects on the antioxidant activity of caffeic and other phenolic acids, *J Agric Food Chem*, 54 (2006) 2932-2937.
- [57] R. Amorati, L. Valgimigli, L. Panzella, A. Napolitano, M. d'Ischia, 5-S-lipoylhydroxytyrosol, a multidefense antioxidant featuring a solvent-tunable peroxy radical-scavenging 3-thio-1,2-dihydroxybenzene motif, *J Org Chem*, 78 (2013) 9857-9864.
- [58] R. Amorati, A. Baschieri, G. Morroni, R. Gambino, L. Valgimigli, Peroxyl Radical Reactions in Water Solution: A Gym for Proton-Coupled Electron-Transfer Theories, *Chemistry*, 22 (2016) 7924-7934.
- [59] W. Zhang, B.R. Johnson, D.E. Suri, J. Martinez, T.D. Bjornsson, Immunohistochemical demonstration of tissue transglutaminase in amyloid plaques, *Acta Neuropathol*, 96 (1998) 395-400.
- [60] B.A. Citron, Z. Suo, K. SantaCruz, P.J. Davies, F. Qin, B.W. Festoff, Protein crosslinking, tissue transglutaminase, alternative splicing and neurodegeneration, *Neurochem Int*, 40 (2002) 69-78.
- [61] S.M. Dudek, G.V. Johnson, Transglutaminase facilitates the formation of polymers of the beta-amyloid peptide, *Brain Res*, 651 (1994) 129-133.
- [62] M.L. Miller, G.V. Johnson, Transglutaminase cross-linking of the tau protein, *J Neurochem*, 65 (1995) 1760-1770.
- [63] J.J. Wakshlag, M.A. Antonyak, J.E. Boehm, K. Boehm, R.A. Cerione, Effects of tissue transglutaminase on beta-amyloid1-42-induced apoptosis, *Protein J*, 25 (2006) 83-94.
- [64] R.R. Ratan, T.H. Murphy, J.M. Baraban, Oxidative stress induces apoptosis in embryonic cortical neurons, *J Neurochem*, 62 (1994) 376-379.
- [65] M. Basso, J. Berlin, L. Xia, S.F. Sleiman, B. Ko, R. Haskew-Layton, E. Kim, M.A. Antonyak, R.A. Cerione, S.E. Iismaa, D. Willis, S. Cho, R.R. Ratan, Transglutaminase inhibition protects against oxidative stress-induced neuronal death downstream of pathological ERK activation, *J Neurosci*, 32 (2012) 6561-6569.
- [66] L. Di, E.H. Kerns, K. Fan, O.J. McConnell, G.T. Carter, High throughput artificial membrane permeability assay for blood-brain barrier, *Eur J Med Chem*, 38 (2003) 223-232.
- [67] E. Nepovimova, J. Korabecny, R. Dolezal, T.D. Nguyen, D. Jun, O. Soukup, M. Pasdiorova, P. Jost, L. Muckova, D. Malinak, L. Gorecki, K. Musilek, K. Kuca, A 7-methoxytacrine-4-pyridinealdoxime hybrid as a novel prophylactic agent with reactivation properties in organophosphate intoxication, *Toxicology Research*, 2016, pp. 1012-1016.
- [68] L.F. Lemes, G. de Andrade Ramos, A.S. de Oliveira, F.M. da Silva, G. de Castro Couto, M. da Silva Boni, M.J. Guimarães, I.N. Souza, M. Bartolini, V. Andrisano, P.C. do Nascimento Nogueira, E.R. Silveira, G.D. Brand, O. Soukup, J. Korábečný, N.C. Romeiro, N.G. Castro, M.L. Bolognesi, L.A. Romeiro, Cardanol-derived AChE inhibitors: Towards the development of dual binding derivatives for Alzheimer's disease, *Eur J Med Chem*, 108 (2016) 687-700.
- [69] H. LeVine, Thioflavine T interaction with synthetic Alzheimer's disease beta-amyloid peptides: detection of amyloid aggregation in solution, *Protein Sci*, 2 (1993) 404-410.
- [70] R. Amorati, L. Valgimigli, P. Dinér, K. Bakhtiari, M. Saeedi, L. Engman, Multi-faceted reactivity of alkyltellurophenols towards peroxy radicals: catalytic antioxidant versus thiol-depletion effect, *Chemistry*, 19 (2013) 7510-7522.
- [71] R. Amorati, J. Zotova, A. Baschieri, L. Valgimigli, Antioxidant Activity of Magnolol and Honokiol: Kinetic and Mechanistic Investigations of Their Reaction with Peroxyl Radicals, *J Org Chem*, 80 (2015) 10651-10659.
- [72] L. Valgimigli, D. Bartolomei, R. Amorati, E. Haidasz, J.J. Hanthorn, S.J. Nara, J. Brinkhorst, D.A. Pratt, 3-Pyridinols and 5-pyrimidinols: Tailor-made for use in synergistic radical-trapping co-antioxidant systems, *Beilstein J Org Chem*, 9 (2013) 2781-2792.
- [73] R. Amorati, G.F. Pedulli, L. Valgimigli, Kinetic and thermodynamic aspects of the chain-breaking antioxidant activity of ascorbic acid derivatives in non-aqueous media, *Org Biomol Chem*, 9 (2011) 3792-3800.
- [74] M.P. Coghlan, A.A. Culbert, D.A. Cross, S.L. Corcoran, J.W. Yates, N.J. Pearce, O.L. Rausch, G.J. Murphy, P.S. Carter, L. Roxbee Cox, D. Mills, M.J. Brown, D. Haigh, R.W. Ward, D.G. Smith, K.J. Murray, A.D. Reith,

- J.C. Holder, Selective small molecule inhibitors of glycogen synthase kinase-3 modulate glycogen metabolism and gene transcription, *Chem Biol*, 7 (2000) 793-803.
- [75] H. Naiki, K. Higuchi, K. Nakakuki, T. Takeda, Kinetic analysis of amyloid fibril polymerization in vitro, *Lab Invest*, 65 (1991) 104-110.
- [76] A. Leblanc, C. Gravel, J. Labelle, J.W. Keillor, Kinetic studies of guinea pig liver transglutaminase reveal a general-base-catalyzed deacylation mechanism, *Biochemistry*, 40 (2001) 8335-8342.
- [77] I. Roy, O. Smith, C.M. Clouthier, J.W. Keillor, Expression, purification and kinetic characterisation of human tissue transglutaminase, *Protein Expr Purif*, 87 (2013) 41-46.
- [78] K. Sugano, H. Hamada, M. Machida, H. Ushio, High throughput prediction of oral absorption: improvement of the composition of the lipid solution used in parallel artificial membrane permeation assay, *J Biomol Screen*, 6 (2001) 189-196.
- [79] F. Wohnsland, B. Faller, High-throughput permeability pH profile and high-throughput alkane/water log P with artificial membranes, *J Med Chem*, 44 (2001) 923-930.

~~Alzheimer's disease is a multifactorial pathology that requires multifaceted agents to address its peculiar nature~~

AD is a pathology that requires multifaceted agents to address its peculiar nature

~~Increasing evidences show that amyloid beta, glycogen synthase kinase 3 β and oxidative stress are strictly intereconnected~~

Increasing evidences show that A β , GSK-3 β and oxidative stress are interconnected

~~Compound 3 demonstrates the ability to inhibit both GSK-3 β and A β_{42} self-aggregation and chelate copper (II)~~

Compound 3 inhibits both GSK-3 β and A β_{42} self-aggregation and chelate copper (II)

~~Compound 3 acts as exceptionally strong radical scavenger in phosphate buffer at pH 7.4 ($k_{inh} = 3.2 \pm 0.5 \cdot 10^5 \text{ M}^{-1} \text{ s}^{-1}$)~~

Compound 3 acts as exceptionally strong radical scavenger at pH 7.4

~~Compound 3 shows low toxicity and neuroprotective effects against toxic insult induced by glutamate~~

Compound 3 shows low toxicity and neuroprotective